Topics in Catalysis
https://doi.org/10.1007/s11244-024-01981-1

ORIGINAL PAPER

Hydrogen Production Came from Catalytic Reforming of Volatiles Generated by Waste-Plastic Pyrolysis Over Sepiolite-Based Catalysts

M. Ángeles Martín-Lara[1] · R. Moreno[1] · G. Blázquez[1] · M. Calero[1]

Accepted: 13 June 2024

Abstract
Several sepiolite-based catalysts have been prepared and investigated for pyrolytic H_2 production from a post-consumer mixture of residual plastics. The experimental installation involved a two-stage reaction system: first, the plastic mixture was thermally pyrolyzed at 500 ºC; then, the generated volatiles were reformed by increasing the temperature to 700 ºC and 800 ºC in the presence of the sepiolite-based catalysts. The real mixture came from non-separate waste collection streams and contained post-consumer polypropylene (rigid and film), expanded polystyrene, high-impact polystyrene, and polyethylene. The results demonstrated that the two-stage pyrolysis technique using sepiolite-based catalysts successfully generated hydrogen. The effects of the type of polymer, temperature, and catalyst were analyzed. The higher production of hydrogen (27.2 mmol H_2/g) was obtained when the mixture of plastic waste was pyrolyzed and then the volatiles were reformed at 800 °C with the SN5-800 12 nickel-modified sepiolite. Additionally, the generation of hydrogen also increased after acidifying natural sepiolite (from 18.2 mmol H_2/g plastic for natural sepiolite to 26.4 mmol H_2/g for acidified sepiolite at 800 ºC with a plastic/catalyst ratio of 1:2). Finally, the carbon deposited in the catalysts was examined. Approximately, only 20% of the carbon that was deposited in the sepiolite-based catalysts was filamentous carbon; the majority was amorphous carbon.

The results have therefore shown that it is possible to obtain a hydrogen-rich gas from the reforming of the pyrolysis vapors of a mixture of plastic waste using a low-cost catalyst based on nickel-modified sepiolite.

Keywords Plastic waste · Hydrogen · Nickel · Catalyst · Sepiolite · Two-stage pyrolysis · Acid treatment

1 Introduction

The industry and society are very interested in plastics as a material. Due to their inherent qualities, they are presently present in all applications [1].

Most plastics are still made today using fossil fuels as raw materials. The conflict in Ukraine in 2022 made the supply chain issues and the high costs of feedstock and energy even worse. The creation of new business models for preventing, reusing, and recycling plastic waste is necessary for the transition to a circular economy, as is the creation of new feedstocks that are easily renewable [2].

In 2022, the total amount of plastic produced climbed to 400.3 million metric tons. Nearly one-third of the world's plastics were produced in China (32.0%). European production rose to 58.7 million metric tons in 2022 (14.6% of the total world's production) [3].

Germany, Italy, France, Spain, Poland, and the United Kingdom had the most demand for plastic converters in Europe in 2021, with more than 3 million metric tons going to packaging (39.1%) and building and construction (21.3%). The most popular plastic is polypropylene (PP), which accounts for 19.8% of demand, followed by low-density polyethylene (LDPE), which accounts for 16.8% of output in Europe [4].

Products produced from plastic materials must be appropriately handled and recycled when their useful lives are

✉ G. Blázquez
gblazque@ugr.es

✉ M. Calero
mcaleroh@ugr.es

M. Ángeles Martín-Lara
marianml@ugr.es

[1] Chemical Engineering Department, Faculty of Sciences, University of Granada, Granada, Spain

Published online: 27 June 2024

finished to recover them and return them to the manufacturing process, promoting the shift to a circular economy [4].

In 2022, 32.3 million metric tons of post-consumer plastic waste were collected in Europe (15.9 million metric tons through mixed waste collection and 16.4 million metric tons through segregated collection). But just 3.8% of the plastics collected through the mixed waste collection program were recycled [5].

Because it cannot be mechanically recycled, mixed or potentially contaminated plastic waste is now landfilled or burned. It is vital to create ecologically friendly waste management methods considering this situation. In this regard, chemical recycling turns into a remedy for this kind of waste [6].

Depending on the chain-breaking agent, there are several different processes utilized to valorize plastic waste via chemical recycling. Thermal cracking, chemical cracking, and biological cracking are the three basic processes [7].

As in the rest of Europe, none of these chemical recycling technologies have been widely adopted at the industrial level in Spain. However, given the large number of businesses interested in undertaking projects of this nature, the rising number of related patents, the diversity of R&I projects being conducted in this field, the vast number of research organizations working on this issue, and the requirement for more recycled plastic materials, among other factors, we are able to forecast a very significant increase in chemical recycling in our nation over the next few years [7].

In thermal cracking, the break of the polymer chain is produced thanks to the action of temperature and, in some cases, by using catalysts. The main processes or techniques are pyrolysis (in the absence of oxygen) and gasification (with oxygen, steam, air, or mixtures of them) [8]. While both pyrolysis and gasification offer sustainable solutions for waste management and energy production, pyrolysis has several advantages over gasification. Firstly, pyrolysis offers a higher yield of valuable by-products such as bio-oil and char compared to gasification. These by-products can be further refined and used as renewable fuels, chemicals, or fertilizers. In addition, pyrolysis operates at lower temperatures, making it a more energy-efficient process compared to gasification. Furthermore, pyrolysis is a versatile technology that can handle a wide range of feedstocks, including agricultural waste, municipal solid waste, and even plastic waste. This makes pyrolysis a more flexible and adaptable solution for waste management and energy production due to its higher yield of valuable by-products and energy efficiency.

The recent advances regarding plastic pyrolysis process introduce various pathways based on the catalyst development. Some previous works presented useful information to further develop and design an advanced catalytic pyrolysis process, with an improved efficiency, desirable product selectivity, and minimum environmental impacts. For this, various catalysts, such as metallic oxides [9], solid acid zeolites (HZSM-5, HY, etc.) [8, 10–12], non-metallic oxides [13–15] or clays [16], have been developed and used to obtain potentially valuable fuels or chemicals.

Special mention has the production of hydrogen from through ex-situ catalytic pyrolysis of plastic waste. Along with renewable energy, renewable-based electrification, and energy efficiency, hydrogen is recognized as a key pillar in the energy transition [17]. Since hydrogen is an energy transporter rather than an energy source, it might play a similar function to electricity in the future. Different energy sources and technologies can create both electricity and hydrogen [18]. In the last few years, the pyrolysis-reforming strategy has been proposed as a suitable route to produce hydrogen from waste plastics [19]. For example, Wu and Williams [20] co-precipitated nickel-based catalysts with different metallic molar ratios to produce hydrogen from the pyrolysis–gasification of PP using a two-stage reaction system. The findings revealed that, regarding hydrogen generation, the catalyst's catalytic activity increased with increasing Ni concentration. Czernik and French [21] analyzed the pyrolysis and catalytic steam reforming of pyrolytic gases and vapours to produce hydrogen from PE and PP in a two-reactor bench-scale system. They reported that, from 60 g/h PP fed to the system, 20.5 g/h hydrogen was produced. Dou et al. [22] proposed a novel system for hydrogen production from plastic waste that combined pyrolysis with CO_2 capture and HCl removal and regeneration of catalysts with carbons deposited. This novel system produced a high-purity hydrogen stream (88.4 vol % of hydrogen). Commercial nickel catalysts were also investigated to convert HDPE and PS into hydrogen using a fluidized bed pyrolysis reactor and in-line reforming. Under optimum conditions, H_2 production was 38.1wt.% and 29.1 wt% for PS [23, 24].

More recently, the combined production of hydrogen and carbon nanotubes over different Ni-based catalysts has also been approached [25, 26]. Wu and Williams [27] analyzed the production of hydrogen using Ni/CeO_2/ZSM-5 catalysts during the two-stage pyrolysis-gasification of PP. The investigation of different Ni contents indicated that, as the Ni content in the catalyst structure was increased, a higher catalytic activity was detected. A high potential for hydrogen production was obtained when the Ni loading was 5 or 10 wt% in the Ni/CeO_2/ZSM-5 catalyst. Also, the SEM photographs of the metal-impregnated catalysts prepared by these authors showed that large amounts of filamentous carbon were formed on the surface of the catalysts [20, 27]. These authors also prepared and investigated several nickel-based catalysts (Ni/Al_2O_3, Ni/MgO, Ni/CeO_2, Ni/ZSM-5, Ni-Al, Ni-Mg-Al and Ni/CeO_2/Al_2O_3) to produce hydrogen

from the two-stage pyrolysis–gasification of polypropylene. The results showed that Ni/ZSM-5 was a good catalyst for hydrogen production, that Ni/Al_2O_3 was deactivated by two types of carbons (monoatomic carbons and filamentous carbons) with a total coke deposition of 11.2 wt% after reaction, although it showed to be an effective catalyst to produce hydrogen and that Ni/MgO showed low catalytic activity for hydrogen production [28]. The same researchers also examined other plastics and their mixtures in a two-stage pyrolysis gasification reactor working with and without Ni-Mg-Al catalyst at temperatures of 800 and 850 ºC. The lowest production of hydrogen was observed for polystyrene (PS) and more filamentous carbons were observed for PP, high-density polyethylene (HDPE) and mixed plastics [29]. Yao et al. [30] processed HDPE using a Ni-zeolite catalyst for hydrogen production. The optimum catalytic performance in terms of hydrogen production was achieved in the presence of the Ni/ZSM5-30 catalyst, with a production of 66.09 mmol of H_2 per gram of HDPE processed.

However, only limited information is available about the pyrolysis of real-world mixed plastic waste collected via mixed waste collection for the production of hydrogen. In addition, the use of low-cost materials abundant in Spain, such as sepiolite, for the preparation of interesting catalysts for the conversion of this real-world mixed plastic waste was not previously investigated. Sepiolite is a naturally occurring clay mineral (fibrous hydrated magnesium silicate) characterized by a favourably specific surface area that has received great consideration as a catalyst support due to its thermal stability and acid-base properties [31]. The use of sepiolite-based catalysts in various industries has been previously proven to significantly improve reaction efficiency and product yield. For example, sepiolite-based catalysts were proven for the selective reduction of nitrogen oxides of copper and nickel [32]. Zhou et al., [33] also tested the photocatalytic activity for the degradation of Orange G of sepiolite-TiO_2 nanocomposites. In addition, Degirmenbasi et al. [34] used sepiolite to synthesized solid base catalysts as a support for transesterification reaction showing good catalytic activity. Special mention has the preparation of sepiolite-supported metal catalysts. In this sense, Han et al. [35] studied sepiolite-supported Ni catalysts for low-temperature CO_2 methanation and found that this new sepiolite-based catalyst showed higher catalytic activity comparing to other Ni-based catalysts. Other researchers investigated the catalytic properties of nickel-sepiolite in hydrogenation of adiponitrile under mild conditions [36].

On the other hand, in other to improve the catalytic activity of sepiolite-based catalysts heat and acid treatment have been studied by many researchers [37–40]. Therefore, in this work, real-world mixed plastic waste collected via mixed waste collection was investigated to produce hydrogen by using sepiolite-based catalysts including nickel modified sepiolite materials. The influence of the effect of acidification of sepiolite, the amount of nickel and the operating temperature on the production of hydrogen was specially investigated.

2 Materials and Methods

2.1 Raw Material

The plastic waste was made up of plastic fragments that a mechanical biological treatment (MBT) facility in Granada (Spain) sent to landfills. High-impact polystyrene (HIPS), rigid and film polypropylene (PP), expanded polystyrene (EPS), rigid polypropylene, and films of other polymers different to PP (non-PP) made up the combination. To ensure homogeneity throughout the pyrolysis test, they were previously separated, cleaned, dried, and submitted to a size reduction procedure (1–3 mm). The raw material obtained had an average composition of 56.10% PP, 12.65% PP film, 12.65% non-PP film, 10.05% EPS, and 8.55% HIPS. To calculate the theoretical H_2 yield, the content in hydrogen of each polymer was determined by elemental analysis in a Thermo Scientific Flash 2000 device. The main results were previously published by Calero et al. [41].

2.2 Preparation and Characterization of the Catalysts

Sepiolite (code S) was supplied by Sigma Alrich. Chemical, structural, and morphological characteristics were stabilized by calcining at 600 ºC for 6 h with air under atmospheric pressure in a Nabertherm, L 3/11/B180 95 Model furnace muffle before being stored in a desiccator. The variables of sepiolite calcination process were chosen accordingly to previous published works [32, 42–45].

A certain amount of acidic sepiolite powder (code SA) was prepared using the formerly calcined sepiolite. The modified sepiolite (code S) was immersed in a 1:10 solution of nitric acid and shaken for 30 min at room temperature. The sample was filtered to remove the water concentration and evaporated to dryness at 120 °C for 3 h. With the sample dry, the SA was spread on a ceramic plate and introduced inside the muffle at 600 ºC for 6 h.

Nickel-modified sepiolites were prepared using the incipient wetness impregnation technique with an aqueous solution of $Ni(NO_3)_2{\cdot}6H_2O$ to load 1 wt% (code SN1) and 5 wt% (code SN5) of nickel. Then, the nickel-modified sepiolites were dried overnight at 105 °C. Finally, the prepared catalysts were calcined at 600 ºC for 6 h in an air environment.

Once the sepiolite-based catalysts were prepared, the textural properties were studied by N_2 physisorption using a Sync 200 device from 3P Instruments©.

In addition, for the chemical composition of the surface, X-ray Photoelectron Spectroscopy (XPS) was carried out in a Kratos AXIS Ultra-DLD device using an X-ray source from Al Kα. All the spectra were corrected to the C1s peak of adventitious carbon to 284.6 eV. For the processing and deconvolution of the peaks, the software XPSpeak 4.1® was used, considering a Shirley background correction.

The disorder degree of carbon was studied by X-ray Diffraction (XRD) in a Bruker D8 Discover device equipped with a detector Pilatus3R 100 K-A, working with Cu Kα radiation (λ = 1.5406 Å). The diffractograms were registered between the 2θ range of 5–80°.

Scan-Transmission Electron Microscopy (STEM-TEM) was used to study catalyst morphology and the distribution of elemental composition with High-Angle Annular Dark Field (STEM HAADF) detection and Electron Disperse X-Ray (Brucker X-flash 6T-30) analysis in a Thermo FisherScientific TALOS F200C G.

After the pyrolysis experiments, the used catalysts were examined using a high-resolution transmission electron microscope (Carl Zeiss STM LIBRA 120 PLUS) to determine the size of the deposition of carbon materials and the surface morphology. Also, temperature-programmed oxidation (TPO) was conducted on a STA 6000 Perkin Elmer thermobalance to evaluate the quality of carbon materials deposited onto the spent catalyst. Around 30 mg of used catalyst were treated with an oxygen flow of 20 mL/min under a temperature program from 30 ºC to 800 ºC at a heating rate of 10 °C/min and a holding time of 10 min at 800 °C.

2.3 Pyrolysis Reactor and Operation Conditions

The plastic waste pyrolysis studies were conducted in a Nabertherm R 50/250/12 Model furnace using a fixed horizontal laboratory-scale stainless steel 316 reactor (internal diameter: 4 cm and length: 34.25 cm). To control the flow of the gas and the cooling of the obtained gas, a flowmeter and a chiller were used.

Table 1 Textural characterization with N_2 adsorption isotherms at 77 K

Material	S_{BET} (m^2/g)	V_T (cm^3/g)
S	108.21	0.48
S-800 12	88.93	0.38
SA	104.56	0.51
SA-800 12	85.93	0.40
SN1	101.88	0.46
SN1-800 12	94.41	0.40
SN5	103.16	0.48
SN5-800 12	98.61	0.42

S_{BET}: Brunauer–Emmett–Teller surface area; V_T: Total pore volume

A closed 316 stainless steel tubular vessel with an internal diameter of 27.25 mm and a length of 30.6 cm and a chimney hole was used to combine 1 g of sample with 1–2 g of catalytic material. The vessel was heated at a rate of 10 ºC/min from room temperature to 700 or 800 ºC, which was maintained for an additional 60 min with a constant flow rate of 0.8 L/min of nitrogen. The reactor was then permanently nitrogen purge cooled to room temperature. A gas sample was collected using TEDLAR bags, and it was separated from the liquid product by a chilling bath at -7 ºC.

The nomenclature of experiments in the following sections was constructed as follows:

First, the code of the catalyst used; second, the temperature of pyrolysis; third, the mass ratio between the amount of plastic waste and the catalytic material. For example, SN5-800 12 is the experiment performed at 800 ºC with nickel-modified sepiolite prepared to get 5 wt% of nickel and with a mass plastic/catalyst ratio of 1/2.

2.4 Gases Analysis

Non-condensed hydrocarbons and gases were determined by using a Micro GC Agilent 990 Bio-Gas analyzer with two channels and thermal conductivity detectors (TCD). Two capillary columns from Agilent J&W Molesieve (5 zeolite molecular sieve, 20 m in length, 0.25 mm in diameter, and a film unit of 30 m) and PoraPLOT Q (Polystyrene-divinylbenzene, 10 m in length, 0.25 mm in diameter, and 8 m of film thickness) were utilized. Backflushes, an injector temperature of 110 ºC, an isothermal oven temperature of 80 ºC, and pressures of 200 and 150 kPa with constant helium flow were the working conditions. Direct injection of the samples was done from TEDLAR bags.

3 Results and Discussion

3.1 Characterization of the Catalysts

Catalyst performance is significantly influenced by pore structure. Table 1 contains a description of the textural characteristics of each catalyst sample (before and after use). All the catalysts had a BET surface area in the range of 85.93 and 123.16 m^2/g and a total pore volume between 0.383 and 0.597 cm^3/g. The BET surface area (S_{BET}) and total pore volume (V_T) decreased after their use in pyrolysis tests due to the deposition of carbon on their surface, as described later in sub-Sect. 3.4. Regarding determination of micropore surface area and micropore volume by using t-plot statistical thickness method, they were zero for all samples. Similar characteristics were reported by other researchers in their studies with sepiolite and metal-modified sepiolite

catalysts. For example, Ardakani et al. [46] obtained a S_{BET} of 116 m^2/g for sepiolite. Also, Suárez and García-Romero [47] collected and characterized 22 samples of sepiolites from different sites and found significant changes in the S_{BET} areas (values between 77 and 399 m^2/g). The results also showed reductions in S_{BET} and V_T for modified sepiolite catalysts (SA, SN1, SN5). In the case of nickel-based sepiolite catalysts, SN1 and SN5 samples, these decreases in the textural parameters can be attributed to the filling of the sepiolite pores with metal particles. This effect on S_{BET} was also reported by Ardakani et al. [46] even in a higher extent in their work about the removal of toluene by cobalt-modified sepiolite, which, for example, reported a S_{BET} of 82 m^2/g for the catalyst with 20 wt% of Co supported on sepiolite compared to 116 m^2/g determined for unmodified sepiolite.

Figure 1 shows the XRD patterns of the catalysts obtained from sepiolite, comparing them with that of natural sepiolite. In the S diffractogram, the structure of the natural sepiolite is identified with its maximum reflections at 8.47º, 20.07º, 28.64º, 34.99º and 38.64º. This mineral has very good crystallinity and showed the characteristic 110 peak of sepiolite (2q = 8.47º) and existence of magnesite (2q = 34.99º) as impurity. After acid treatment with HCl (SA diffractogram in Fig. 1) the intensities of the sepiolite reflections in 8.5º, 10.7º and 17.5º disappeared with respect to the natural mineral. These results show the acid reduce the crystallinity of the sepiolite although it still presents good crystallinity. The SN1 and SN5 diffractograms represent the results of the nickel-based catalyst supported on sepiolite. A decrease in crystallinity is recognized with respect to the natural sample. Furthermore, the catalyst samples exhibit the same characteristic peaks at 37.2°, 43,1° and 62.5°, which were assigned to NiO [48]. Finally, if the diffractograms of the SN5 samples before and after the pyrolysis test are compared, no notable differences have been observed between the results obtained.

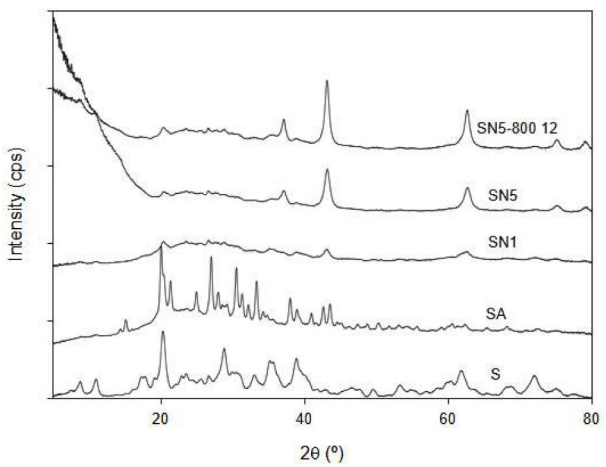

Fig. 1 XDR patterns of the catalysts

XPS was also applied to characterize the surface of the catalysts in terms of chemical composition, nature, and electronic structure of the surface of nickel-impregnated sepiolite before and after their use in the pyrolysis tests. High resolution XPS deconvolution spectra are shown in Fig. 2 and the distribution of main peaks and their contributing areas in Table 2.

The Si_{2p} core level spectrum was divided into four possible contributions in both samples, mainly: Si_3N_4 (101.7 eV), organic Si (~ 102 eV), dominant Si in the magnesium silicate framework (102.7 eV), and surface SiO_2 (103.5 eV). No significant changes in surface Si distribution were observed upon pyrolysis, except for contribution of Si in the magnesium silicate framework due to lower area after use.

The Mg_{1s} spectrum was decomposed into two main components at binding energies placed at 1303.0 eV and 1304.5 eV. The most intense absorption at 1303 eV was associated with metal Mg in the sepiolite structure which constituted over 90% of the total Mg at the surface.

The O_{1s} core level spectra identified four components in sepiolite, with energies ranging from 529.0 eV to 532.9 eV. These components include single bond oxygens interacting with metals (529–530 eV), structural hydroxyl groups linked to Mg sites (531.7 eV), silicate framework oxygens (532.9 eV) and the most intense line at 531.1 eV that is covered by the contribution from metal oxides [49].

The Ni_{2p} showed a complex spectra with multiple-split peaks at binding energies of the following chemical states: $Ni_{2p1/2}$ satellite ($Ni(OH_2)$ and NiO) at approximately respectively 880 eV and 872 eV, $Ni_{2p1/2}$ attributable to Ni metal at approximately 870 eV, $Ni_{2p3/2}$ satellite ($Ni(OH_2)$ and NiO) at approximately 860 eV, multiple-split $Ni_{2p3/2}$ (NiO) and $Ni_{2p3/2}$ (Ni metal) at approximately 855 and 854 eV. No significative differences were observed between the sample before and after pyrolysis.

Finally, Table 3 reports the quantification of XPS spectra showing real nickel mass concentrations on Ni-modified sepiolite samples.

TEM micrographs of SN5 samples before (SN5) and after pyrolysis tests (SN5-800 12) are shown in Fig. 3a and d. Roughly nickel oxide particles are visible in these micrographs (dark dots), especially in Fig. 3c and d where, in addition, slightly nickel agglomerations can be detected. Also, the element mapping images (Fig. 3e and f) illustrate the uniform distribution of Mg (red), Si (blue) and Ni (green) elements on both sepiolite surface. These results are agreed with these found by other researchers as Lv et al. [50] who prepared nickel and potassium bimetallic catalysts supported on acid-activated sepiolite for 1,6-hexanedinitrile

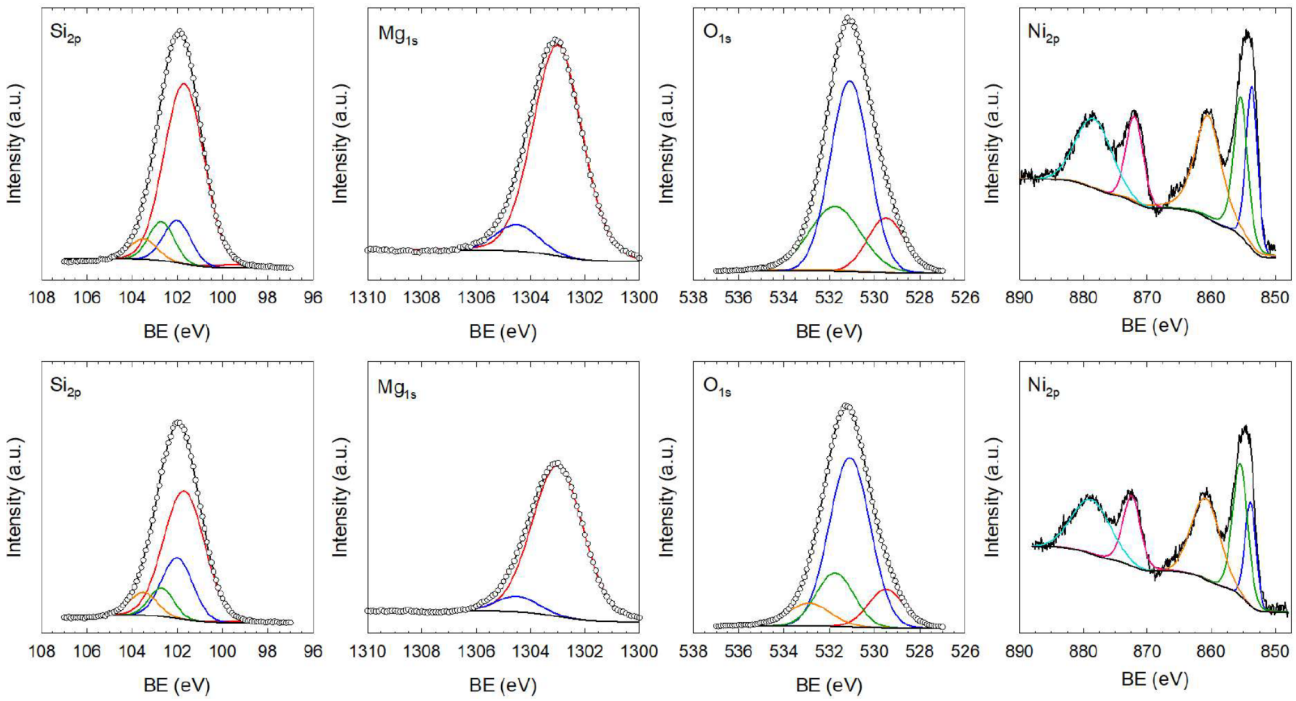

Fig. 2 High resolution XPS deconvolution spectra of fresh (up subfigures) and used (down subfigures) nickel-sepiolite samples

Table 2 Distribution of main peaks and their contributing areas

Element	Peak	Before		After	
		Raw Area (cps eV)	% Area	Raw Area (cps eV)	% Area
Si	99.4 eV	418	1.3%	181	0.6%
	101.7 eV	24,012	71.9%	17,645	61.8%
	102.0 eV	3861	11.6%	6324	22.1%
	102.7 eV	3275	9.8%	2320	8.1%
	103.5 eV	1838	5.5%	2090	7.3%
Mg	1303 eV	69,892	90.6%	51,840	92.5%
	1304.5 eV	7256	9.4%	4178	7.5%
O	529.5 eV	33,326	15.9%	22,602	12.2%
	531.1 eV	119,371	56.9%	113,037	61.2%
	531.7 eV	56,098	26.7%	32,806	17.8%
	532.9 eV	1132	0.5%	16,118	8.7%
Ni	824.1 eV	2200	8.3%	7606	25.1%
	853.8 eV	4674	17.7%	3234	10.7%
	855.5 eV	3735	14.1%	4590	15.1%
	860.6 eV	7306	27.6%	6639	21.9%
	872.2 eV	3143	11.9%	3007	9.9%
	878.5 eV	5373	20.3%	5250	17.3%

hydrogenation and Chen et al. [51] who synthetized sepiolite/amorphous nickel hydroxide for its use as supercapacitor.

3.2 Gas Compositions

3.2.1 Comparison Between Polymers

Figure 4 shows the composition of gases as a function of the polymer pyrolyzed. The type of polymer greatly affects the gas composition. Rigid PP waste provided the highest hydrogen percentage, followed by HIPS and EPS (both PS waste). Regarding methane, their percentage on gases was higher for gases obtained from the pyrolysis of film waste and the mixture of plastics. Another important compound in gases was carbon monoxide, which showed a similar percentage in all obtained gases.

Regarding the effect of the pyrolysis temperature, the hydrogen and carbon monoxide content increased with the increase in temperature. For example, the hydrogen content was 19.59% at 700 °C and increased to 43.20% at 800 °C for the mixture of plastics, and the carbon monoxide was 15.41% at 700 ºC and increased to 27.22% at 800 ºC for HIPS waste. However, methane and ethane decreased as the

Table 3 Quantification of XPS spectra

	O 1s		Si 2p		C 1s		Mg 1s		Ni 2p	
	Before	After	Before	After	Before	After	Before	After	Before	After
Raw Area (cps eV)	739,717	692,633	101,772	90,726	35,369	51,152	171,914	119,498	123,631	105,860
Atomic Conc %	63.52	62.32	19.53	18.24	8.37	12.68	5.66	4.12	2.07	1.85
Mass Conc %	52.36	52.86	28.26	27.16	5.18	8.07	7.09	5.31	6.25	5.77

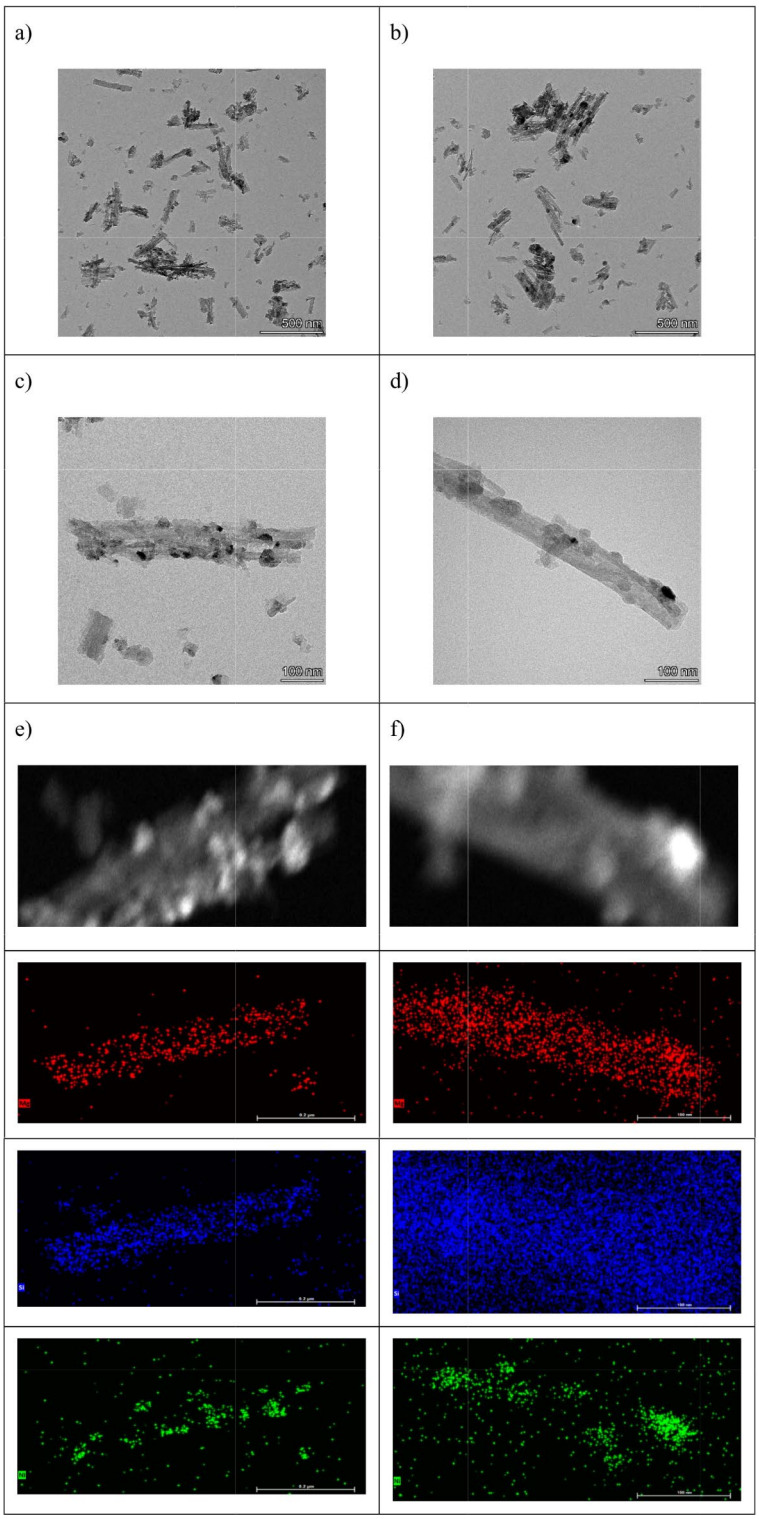

Fig. 3 TEM images of (**a**) SN5, (**b**) SN5-800 12, (**c**) SN5 and (**d**) SN5-800 12 and EDS images of (**e**) SN5 and (**f**) SN5-800 12

temperature increased. For example, the methane percentage changed from values between 11.36 and 38.67% at 700 ºC to 4.94–22.70% at 800 ºC.

Many reactions can take place in the thermal cracking process. Some of these reactions favour the production of hydrogen, especially at elevated temperatures. In contrast to hydrogen, other components could increase or decrease depending on the extent of the secondary reactions. For example, other authors have reported the increase of H_2 concentrations as the reaction temperature was raised from 600 to 750 °C and CH_4 and C2 – C5 hydrocarbon concentrations decreases due to the enhancement in the dry reforming of

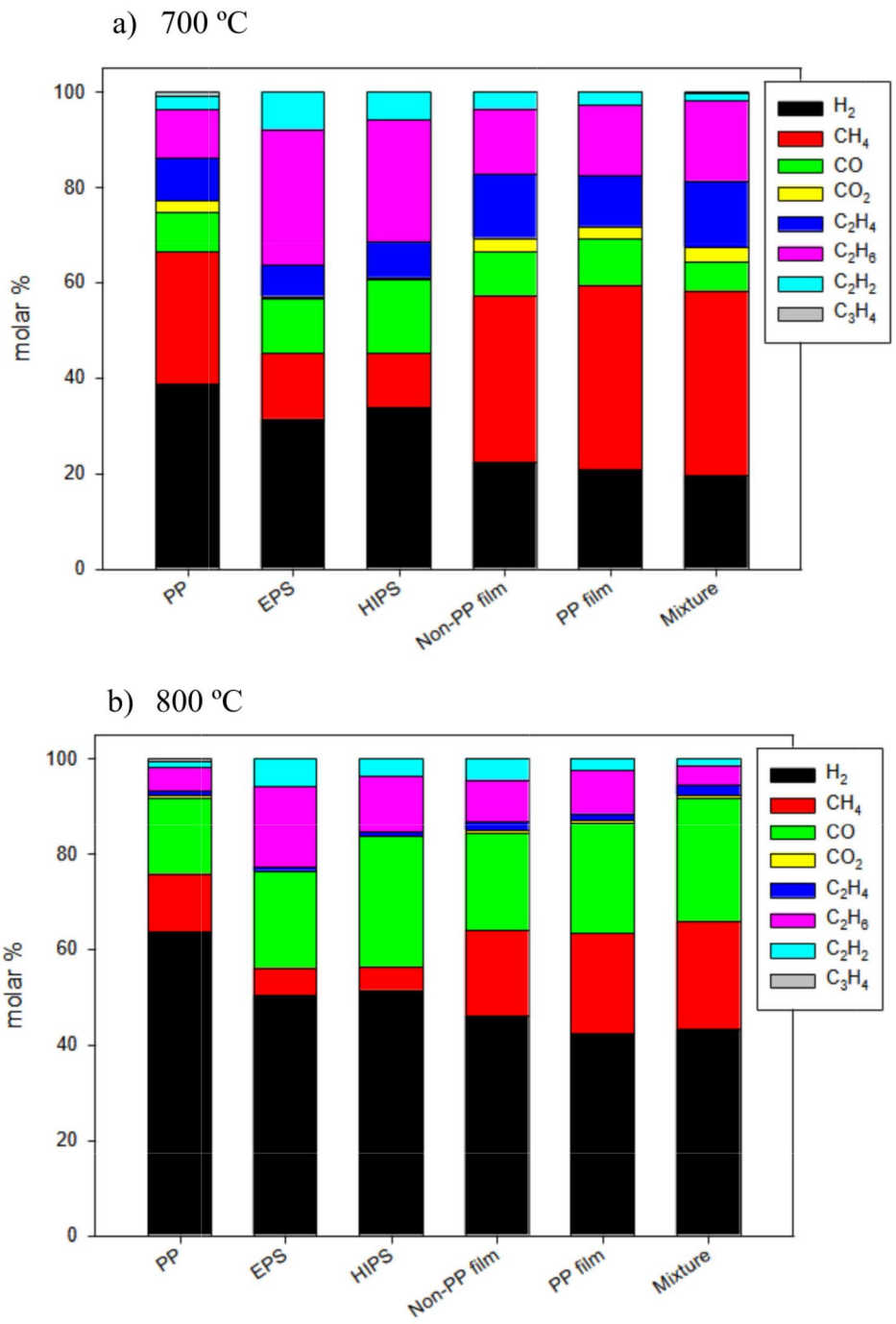

Fig. 4 Molar composition of gases in function of polymer pyrolyzed

CH_4, dry reforming of hydrocarbons, and direct decomposition of hydrocarbons [52]. Some of the main involved reactions are summarized below:

$$\text{Tar} \rightarrow CH_4 + H_2O + C_mH_n + H_2.$$
$$CH_4 + H_2O \rightarrow CO + 3H_2.$$
$$C + H_2O \rightarrow CO + H_2.$$
$$CO + H_2O \rightarrow CO_2 + H_2.$$
$$C + CO_2 \rightarrow 2CO.$$
$$C + 2H_2 \rightarrow CH_4.$$
$$CH_4 + CO_2 \rightarrow 2CO + 2H_2.$$
$$C_mH_n + 2nH_2O \rightarrow nCO_2 + [2n + (m / 2)]H_2.$$
$$C_mH_n + nH_2O \rightarrow nCO + [n + (m / 2)]H_2.$$

To better describe the effect of the type of polymer and pyrolysis temperature on the production of hydrogen, the experimental, theoretical, and experimental/theoretical ratios of H_2 yields were calculated and reported in Table 4.

The higher theoretical H_2 yield was obtained for PP polymer followed by EPS and HIPS materials. Particularly, a maximum hydrogen yield of 75.4 mmol of H_2 per g of plastic was calculated for rigid PP plastic. If theoretical H_2 yield

Table 4 Experimental, theoretical, and experimental/theoretical ratios of H_2 yields in function of polymer pyrolyzed

Material	Temperature (ºC)	Experimental H_2 yield (mmol/g)	Theoretical H_2 yield (mmol/g)	Experimental/theorical ratio (%)
PP	700	10.66	75.40	14.14
	800	29.06		38.55
EPS	700	2.80	48.30	5.79
	800	15.22		31.51
HIPS	700	2.67	40.75	6.56
	800	14.49		35.56
Non-PP film	700	3.49	37.50	9.31
	800	14.51		38.68
PP film	700	3.15	72.50	4.35
	800	22.53		31.08
Mixture	700	6.17	65.09	9.47
	800	16.33		25.08

values are compared with experimental data, ratios between 4.35 (PP film at 700 ºC) and 38.68 (Non-PP film at 800 ºC) were calculated. In general, experimental/theorical H_2 yield ratios were in the range of 4–15 at 700 ºC and in the range of 30–40 at 800 ºC. These results indicated a positive effect of temperature on the production of hydrogen and better performance of PP samples since this polymer presented higher experimental/theorical H_2 yield ratios at both investigated temperatures. Other authors have previously informed that the formation of hydrogen is enhanced due to cracking of hydrocarbons into smaller fragments at higher temperatures [23].

Williams [26] indicates that the influence of the type of plastic in terms of hydrogen production is very significant, since it depends on the different decomposition products obtained in the pyrolysis of each type of material. For example, pyrolysis of polyethylene and polypropylene will produce mainly long and short chain linear and branched alkanes and alkenes, while polystyrene will produce mainly styrene and styrene oligomers. These different volatiles will give rise to different compounds in the reforming process, thus influencing the production of hydrogen. Wu and Williams [29] obtained different hydrogen production rates in the pyrolysis of various types of plastics at 800 and 850 ºC without the use of a catalyst. These authors found H_2 yields corresponding to the mass of raw plastic of 6, 7 and 26 gH_2/gplastic for PP, PS, and HDPE, respectively, at 800 ºC and of 26, 10.5 and 34 gH_2/gplastic for PP, PS, and HDEP, respectively, at 850 ºC.

3.2.2 Comparison Between Catalysts

Figure 5 shows the composition of gases as a function of the catalyst used and temperature for the mixture of plastics. Important increases in H_2 and CO molar percentages were observed when the temperature was changed from 700 ºC to 800 ºC. However, the analysis of the temperature impact showed that an increase in temperature decreased the C_2 contents, which were significantly lower than those of H_2, CH_4, and CO, indicating especially that the increase in temperature is favourable for the generation of H_2.

Regarding the impact of the studied catalysts, the use of sepiolite-based catalysts as an additive in the tar cracking zone provided higher hydrogen production compared to pyrolysis without a catalyst.

The relative content of H_2 in the absence of the catalysts was 19.59% at 700 ºC and 43.20% at 800 ºC, lower than those percentages in the presence of the sepiolite-based catalysts. Increases were especially distinguished for Ni-modified sepiolite; also, as the plastic-catalyst ratio and Ni content increased, the relative content of H_2 increased, for example, from 47.79 to 60.37% if SN1-800 11 and SN5-800 12 were compared. Moreover, when the relative content of H_2 increased, the proportion of CH_4 decreased.

To better describe the effect of the type of catalyst and pyrolysis temperature on the production of hydrogen, the experimental and experimental/theoretical ratio of H_2 yields were calculated and reported in Table 5.

The effects of sepiolite were only notable at 800 ºC and specially with mass plastic/catalyst ratio of 1/2. In addition, under the analyzed reaction conditions, unmodified sepiolite did not show any increase in H_2 production, even a slight decrease. However, the experimental H_2 yield obtained with acidified and Ni-modified sepiolite was increased at 800 ºC. For example, an experiment performed with Ni-modified sepiolite with 5% of nickel and a plastic/catalyst ratio of 1/2 showed a H_2 production of 27.210 mmol/g higher than 16.327 mmol/g obtained in thermal pyrolysis (without catalyst at the same temperature of 800 ºC). Finally, although the Ni-modified catalysts increased their capacity to produce hydrogen as the ratio of Ni increased, with catalyst 5% Ni having the better hydrogen yield, this effect was not especially important. Although some studies have analyzed nickel loadings ranging between 0 and 50 wt% [53–55], some other previous reports have shown that low Ni loadings leading to a positive effect on the catalytic capacity of the nickel-based prepared materials. For example, Pham et al. [56], examined methane dry reforming using nickel-based alumina catalysts with a metal dosage ranging from 0.5 to 3 wt% and the presence of active metal showed a great impact at the beginning leading to big improvements in feedstock conversion. In addition, beyond a nickel dosage of 2 wt%, further additions did not noticeably influence the reaction performance. Also, effect of nickel loading on hydrogen adsorption capacity of different mesoporous supports was examined by Carraro et al., [57] and the results showed that nickel loadings of 2.5 wt% was capable to

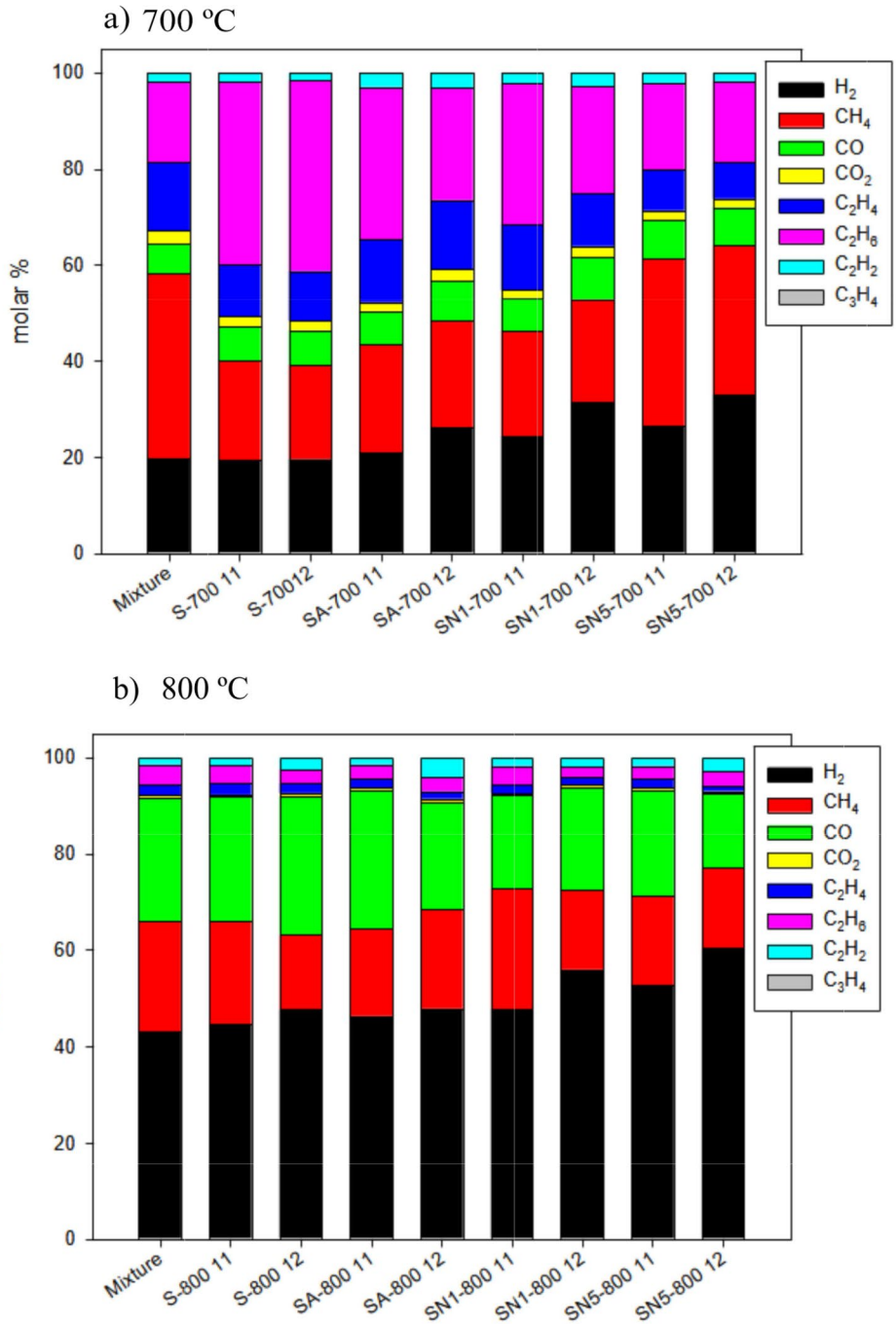

Fig. 5 Molar composition of gases in function of the catalyst used

enhancing the hydrogen adsorption capacity. Thus, the aim of this study was evaluating the low nickel loading over sepiolite support on the hydrogen production by pyrolysis of plastic waste. Currently, to our best knowledge, although nickel catalyst which is traditionally used for hydrogen production, little information could be found on the investigation of low loading nickel on the production of hydrogen from pyrolysis of plastics. In addition, if results reported in Table 5 are deeply examined an increase in nickel loading (between 1% and 5%) was not produced an important improvement in H_2 production to justify the use of higher nickel loading concentrations.

Prior research has examined the use of catalysts in the pyrolysis of plastic waste to produce hydrogen, with most catalysts' active elements being transition metals [58]. In the case of nickel, a transition metal with good catalytic action and reasonable cost when compared to other precious metals, several authors have confirmed its great hydrogen selectivity. For example, Liu et al. [59] obtained a value of 22.60 mmol H_2/g from the catalytic gasification of PP by using

Table 5 Experimental, theoretical, and experimental/theoretical ratios of H_2 yields in function of catalyst used

Catalyst	Experimental H_2 yield (mmol/g)	Theoretical H_2 yield (mmol/g)	Experimental/theoretical ratio (%)
Without catalyst-700	6.17	65.09	9.47
Without catalyst-800	16.33		25.08
S-700 11	5.14		7.90
S-800 11	16.01		24.60
S-700 12	5.31		8.16
S-800 12	18.15		27.88
SA-700 11	5.48		8.41
SA-800 11	23.14		35.56
SA-700 12	6.33		9.72
SA-800 12	26.43		40.61
SN1-700 11	6.78		10.42
SN1-800 11	22.68		34.85
SN1-700 12	12.99		19.96
SN1-800 12	26.63		40.92
SN5-700 11	9.71		14.92
SN5-800 11	26.87		41.29
SN5-700 12	14.75		22.66
SN5-800 12	27.21		41.80

Ni/SiO_2 catalysts with different metal particle sizes. Also, a yield of hydrogen of 31.8 mmol H_2/g plastic was obtained by Yao et al. [48] in the pyrolysis of a mixture of plastics over the Ni-Fe/γ-Al_2O_3 catalyst at 800 °C. More recently, Li et al. [60] examined the pyrolytic catalysis of polyethylene (PE) to hydrogen and reported that Ni-modified ZSM-5 generated a hydrogen production of 26.27 mmol H_2/g. Xu et al. [61] also investigated the pyrolysis of biomass and PE using Ni-pine sawdust as catalyst at temperatures ranged between 600 and 800 °C and obtaining 42.28 mmol of H_2 by g feedstock. Also, Alvarez et al. [62] examined the catalytic pyrolysis of pinewood sawdust and PP using Ni–Al_2O_3 as catalyst at the same temperatures and reported a production of H_2 of 27.27 mmol/g. Finally, Wang et al., [63] investigated the production of H_2 by pyrolysis of PP using Ni-activated carbon at 500–900 °C and found 40.24 mmol/g.

Regarding catalytic mechanism, first, plastic waste is pyrolyzed to produce a variety of hydrocarbons, which serve as precursors for carbon and hydrogen in later nickel reforming step. Nickel active catalysts divided these hydrocarbons into smaller free radicals, which then recombine close to the active site to create gaseous products that are mostly hydrogen [63]. Specific reactions were described before in subsection 3.3.1.

According to the results obtained in this work, similar performance in terms of H_2 production (mmol H_2/g plastic) was obtained for SA, SN1 and SN5 samples. Between SN1 and SN5 authors proposed the use of a lower nickel amount to avoid the use of metals and between SA and SN1 samples a comparative life cycle assessment of catalyst synthesis processes should be performed to examine environmental impacts derived to formation of wastes that mainly comprise liquid waste and energetic consumptions, between others, before to propose the better catalyst.

3.3 Characterization of Carbon Depositions

3.3.1 TEM Analysis

In Fig. 6, TEM micrographs of the examined catalysts were displayed. All the catalysts used had similar patterns with nano-sized sections and long lengths. Since sepiolite fibre is micrometric in length and nanometric in section and frequently appearing grouped, it is very difficult to distinguish the presence of carbon nanostructures and their individual sizes. S-800 12 catalyst showed a higher dispersion of sepiolite nanostructures in all the material and SA-800 12, SN1-800 12 and SN5-800 12 showed a greater agglomeration perhaps to higher deposition of carbons. Numerous researchers have investigated the production of carbon nanostructures from waste plastics [64–66]. For example, Bazargan and McKay [67] reviewed published works that use the pyrolysis of plastics to synthesize carbon nanostructures and organized the results in terms of reactor design. More recently, Williams [26] examined the impact of reactor and catalyst type on the yield and quality of the produced carbon nanotubes. Regarding the use of nickel-based catalysts, some authors, such as Mishra et al. [68], found carbon nanotubes in the polypropylene pyrolysis using nickel as a catalyst. The authors found carbon nanotubes in the range of 25 nm with Ni metal in the centre of the tube. Other researchers [69] observed similar results, reporting filamentous carbons with outer diameters between 10 and 30 nm and metal particles wrapped in the tubes in the pyrolysis of polypropylene using Ni- and Fe-based catalysts.

3.3.2 TPO Analysis

Also, temperature-programmed oxidation (TPO) analysis was used to ascertain the different thermal degrading properties of carbon placed on used catalysts. The findings summarized in Fig. 7; Table 6. Figure 7 shows the proportions of amorphous and filamentous types of carbon deposited on catalysts. The data were obtained from thermogravimetric curves (data here not shown) analyzing the different steps of weight loss. According to the relevant literature, the weight loss that occurred between 400 and 800 °C was due to the oxidation of carbon components that have been deposited on the catalyst [60] and depending on temperature at which weight loss was completed the various carbon types can be distinguished [70]. The weight loss at low temperature

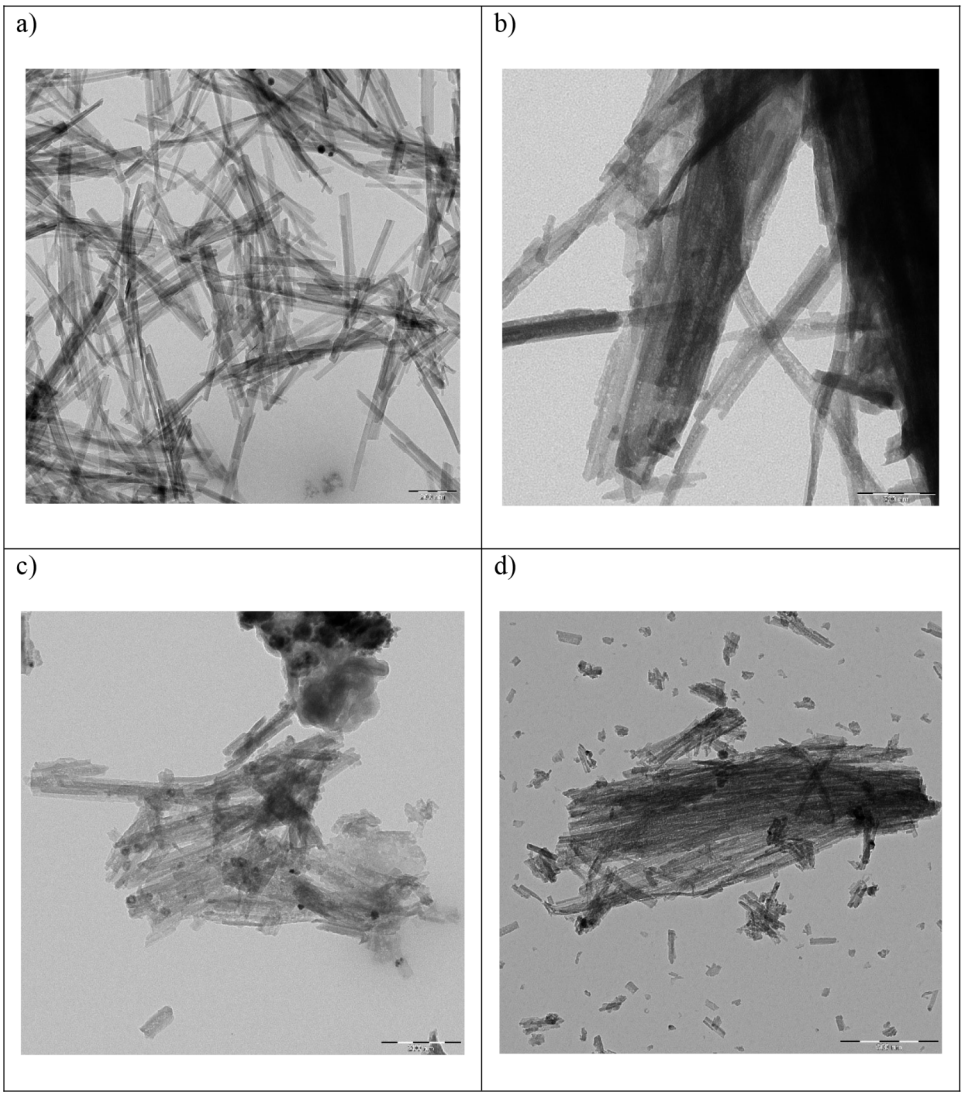

Fig. 6 TEM micrographs of used catalysts after pyrolysis. (**a**) S-800 12, (**b**) SA-800 12, (**c**) SN1-800 12, (**d**) SN-5 800 12

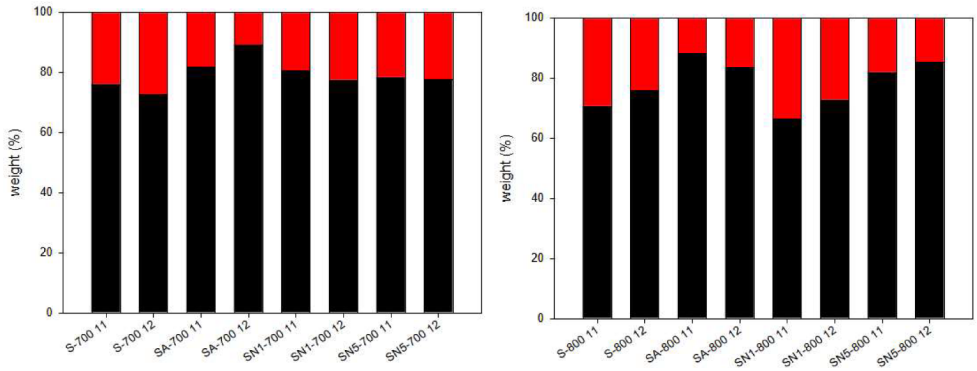

Fig. 7 Weight% of amorphous (black colour) and filamentous (red colour) carbon materials

(around 400 and 600 °C) was ascribed to the more unstable amorphous carbon, whereas the weight loss at high temperature (more than 600 ºC) was linked to the oxidation of the more thermally stable filamentous carbon materials [71]. A larger percentage of amorphous carbon (over 80%) was found in carbon deposits from most catalysts. Due to the limited specific surface area and porosity of these catalysts, perhaps the internal dispersion of the metal-active particles is poor, which can justify the high production of amorphous carbon [50]. Previous works have shown that a weak metal-support interaction results in more amorphous carbons and less filamentous carbon [72]. These authors suggested that

Table 6 Carbon deposition (mg carbon by gram of catalyst) in function of pyrolysis temperature, dosage of plastic: catalyst and catalyst sample

Catalyst sample	Temperature, ºC	Dosage (wt: wt.) plastic: catalyst	Carbon deposition, mg/g
S	700	1:1	22.48
		1:2	20.22
	800	1:1	26.59
		1:2	33.98
SA	700	1:1	67.54
		1:2	73.10
	800	1:1	145.05
		1:2	122.57
SN1	700	1:1	17.87
		1:2	59.79
	800	1:1	34.24
		1:2	71.41
SN5	700	1:1	53.50
		1:2	30.97
	800	1:1	69.49
		1:2	71.48

the interaction between the metal and support played a strong part in governing the yield and type of carbon, with a too weak interaction producing particles too large for filamentous carbon growth.

According to previous papers, since hydrogen is given off during carbon deposition, a larger amount of carbon would result in a corresponding high yield in hydrogen [72, 73]. Table 6 reported the total carbon deposition (evaluated in mg of carbon by gram of catalyst) in function of pyrolysis temperature, dosage of plastic catalyst and catalyst sample. If carbon deposition data are compared with experimental H_2 production data, in general, a slight linear correlation can be found between them for each different catalyst sample.

4 Conclusions

In this work, the hydrogen production came from the catalytic reforming of volatiles generated by waste-plastic pyrolysis over sepiolite-based catalysts was explored. The findings indicated that the type of polymer greatly affects the gas composition, with rigid PP waste providing the highest hydrogen yield (39.06 mmol/g). Regarding the effect of the pyrolysis temperature, results indicated a positive effect of temperature on the production of hydrogen since hydrogen production was raised with the increase in temperature from 700 ºC to 800 ºC. A comparison between catalysts showed that nickel-modified sepiolite samples work well as catalysts for the generation of hydrogen, reaching 41.8% of the theoretical hydrogen potential. Finally, the characterization of carbon deposited over catalysts' surfaces showed that most of the carbons were amorphous, with no significant differences between the catalysts. Also, total carbon deposition was evaluated, obtaining values ranging between 17.87 and 145.05 mg/g in function of pyrolysis temperature, dose of plastic-catalyst and type of catalyst sample.

Acknowledgements This project has been financed by FEDER/Junta de Andalucía-Ministry of Economic Transformation, Industry, Knowledge, and Universities, Project P20_00167. Funding for open access charge: University of Granada/CBUA.

Funding Funding for open access publishing: Universidad de Granada/CBUA.

References

1. Bucknall DG (2020) Plastics as a materials system in a circular economy. Phil Trans R Soc A 378:20190268. https://doi.org/10.1098/rsta.2019.0268
2. European Environmental Agency (2023) Pathways towards circular plastics in Europe — good practice examples from countries, business and citizens. https://www.eea.europa.eu/publications/pathways-towards-circular-plastics-in
3. Plastics Europe. Plastics-The Facts (2023) https://plasticseurope.org/knowledge-hub/plastics-the-fast-facts-2023/
4. Plastics Europe. Plastics-The Facts (2022a) https://plasticseurope.org/knowledge-hub/plastics-the-facts-2022/
5. Plastics Europe. The Circular Economy for Plastics. A European Analysis (2024) https://plasticseurope.org/resources/market-data/
6. Pacheco-López A, Gómez-Reyes E, Graells M, Espuña A, Somoza-Tornos A (2023) Integrated synthesis, modelling, and assessment (iSMA) of waste-to-resource alternatives towards a circular economy: the case of the chemical recycling of plastic waste management. Comput Chem Eng 175:108255. https://doi.org/10.1016/j.compchemeng.2023.108255
7. Plastics Europe (2022b) Chemical Recycling in Spain: Fostering a Circular Future. Report conducted by AIMPLAS. https://plasticseurope.org/wp-content/uploads/2022/09/Informe-RQ-2021-ING-A4.pdf
8. Papuga S, Djurdjevic M, Ciccioli A, Vecchio Ciprioti S (2023) Catalytic Pyrolysis of Plastic Waste and Molecular Symmetry effects: a review. Symmetry 15:38. https://doi.org/10.3390/sym15010038
9. Cai N, Xia S, Li X, Xiao H, Chen X, Chen Y, Bartocci P, Chen H, Williams PT, Yang H (2021) High-value products from ex-situ catalytic pyrolysis of polypropylene waste using iron-based

catalysts: the influence of support materials. Waste Manag 136:47–56. https://doi.org/10.1016/j.wasman.2021.09.030
10. Akin O, Varghese RJ, Eschenbacher A, Oenema J, Abbas-Abadi MS, Stefanidis GD, Van Geem KM (2023) Chemical recycling of plastic waste to monomers: effect of catalyst contact time, acidity and pore size on olefin recovery in ex-situ catalytic pyrolysis of polyolefin waste. J Anal Appl Pyrol 172:106036. https://doi.org/10.1016/j.jaap.2023.106036
11. Paucar-Sánchez MF, Calero M, Blázquez G, Solís RR, Muñoz-Batista MJ, Martín-Lara MA (2022) Thermal and catalytic pyrolysis of a real mixture of post-consumer plastic waste: an analysis of the gasoline-range product. Process Saf Environ Prot 168:1201–1211. https://doi.org/10.1016/j.psep.2022.11.009
12. Quesada L, Calero M, Martín-Lara MÁ, Pérez A, Paucar-Sánchez MF, Blázquez G (2022) Characterization of the different oils obtained through the Catalytic In Situ Pyrolysis of Polyethylene Film from Municipal Solid Waste. Appl Sci 12:4043. https://doi.org/10.3390/app12084043
13. Fan L, ZhangY, Liu S, Zhou N, Chen P, Liu Y, Wang Y, Peng P, Cheng Y, Addy M, Lei H, Ruan R (2017) Ex-situ catalytic upgrading of vapors from microwave-assisted pyrolysis of low-density polyethylene with MgO. Energy Conv Manag 149:432–441. https://doi.org/10.1016/j.enconman.2017.07.039
14. Yuan R, Shen Y (2019) Catalytic pyrolysis of biomass-plastic wastes in the presence of MgO and MgCO3 for hydrocarbon-rich oils production. Bioresour Technol 293:122076. https://doi.org/10.1016/j.biortech.2019.122076
15. Sophonrat N, Sandström K, Svanberg R, Han T, Dvinskikh S, Lousada CM, Yang W (2019) Ex situ Catalytic pyrolysis of a mixture of polyvinyl chloride and cellulose using calcium oxide for HCl adsorption and Catalytic Reforming of the Pyrolysis products. Ind Eng Chem Res 58:3960–13970. https://doi.org/10.1021/acs.iecr.9b02299
16. Cai W, Kumar R, Zheng Y, Zhu Z, Wong JWC, Zhao J (2023) Exploring the potential of clay catalysts in catalytic pyrolysis of mixed plastic waste for fuel and energy recovery. Helyon 9:e23140. https://doi.org/10.1016/j.heliyon.2023.e23140
17. World energy transitions outlook 2022: 1.5°C pathway, International Renewable Energy Agency, Abu IRENA, Dhabi (2022a) https://www.irena.org/publications/2022/Mar/World-Energy-Transitions-Outlook-2022
18. Yue M, Lambert H, Pahon E, Roche R, Jemei S, Hissel D (2021) Hydrogen energy systems: a critical review of technologies, applications, trends and challenges. Renew Sustain Energy Rev 146:111180. https://doi.org/10.1016/j.rser.2021.111180
19. Cortazar M, Gao N, Quan C, Suarez MA, Lopez G, Orozco S, Santamaria L, Amutio M, Olazar M (2022) Analysis of hydrogen production potential from waste plastics by pyrolysis and in line oxidative steam reforming. Fuel Processing Technology. 225:107044. https://doi.org/10.1016/j.fuproc.2021.107044
20. Wu C, Williams PT (2009) Investigation of Ni-Al, Ni-Mg-Al and Ni-Cu-Al catalyst for hydrogen production from pyrolysis–gasification of polypropylene. Appl Catal B 90:147–156. https://doi.org/10.1016/j.apcatb.2009.03.004
21. Czernik S, French RJ (2006) Production of Hydrogen from Plastics by Pyrolysis and Catalytic Steam Reform. Energy Fuels 20:754–758. https://doi.org/10.1021/ef050354h
22. Dou B, Wang K, Jia ng B, Song Y, Zhang C, Chen H, Xu Y (2016) Fluidized-bed gasification combined continuous sorption-enhanced steam reforming system to continuous hydrogen production from waste plastic. Int J Hydrog Energy 41:3803–3810. https://doi.org/10.1016/j.ijhydene.2015.12.197
23. Barbarias I, Lopez G, Alvarez J, Artetxe M, Arregi A, Bilbao J, Olazar MA (2016) Sequential process for hydrogen production based on continuous HDPE fast pyrolysis and in-line steam reforming. Chem Eng J 296:191–198. https://doi.org/10.1016/j.cej.2016.03.091
24. Barbarias I, Lopez G, Artetxe M, Arregi A, Santamaria L, Bilbao J, Olazar M (2016) Pyrolysis and in-line catalytic steam reforming of polystyrene through a two-step reaction system. J Anal Appl Pyrol 122:502–510. https://doi.org/10.1016/j.jaap.2016.10.006
25. Sharma SS, Batra VS (2020) Production of hydrogen and carbon nanotubes via catalytic thermo-chemical conversion of plastic waste: review. J Chem Technol Biotechnol 95:11–19. https://doi.org/10.1002/jctb.6193
26. Williams PT (2021) Hydrogen and Carbon nanotubes from Pyrolysis-Catalysis of Waste Plastics: a review. Waste Biomass Valor 12:1–28. https://doi.org/10.1007/s12649-020-01054-w
27. Wu C, Williams PT (2009) Ni/CeO_2/ZSM-5 catalysts for the production of hydrogen from the pyrolysis–gasification of polypropylene. Int J Hydrog Energy 34:6242–6252. https://doi.org/10.1016/j.ijhydene.2009.05.121
28. Wu C, Williams PT (2009) Hydrogen production by steam gasification of polypropylene with various nickel catalysts. Appl Catal B 87:152–161. https://doi.org/10.1016/j.apcatb.2008.09.003
29. Wu C, Williams PT (2010) Pyrolysis–gasification of plastics, mixed plastics and real-world plastic waste with and without Ni–Mg–Al catalyst. Fuel 89:3022–3032. https://doi.org/10.1016/j.fuel.2010.05.032
30. Yao D, Yang H, Chen H, Williams PT (2018) Investigation of nickel-impregnated zeolite catalysts for hydrogen/syngas production from the catalytic reforming of waste polyethylene. Appl Catal B 227:477–487. https://doi.org/10.1016/j.apcatb.2018.01.050
31. Ortega F, Martín-Lara MA, Pula HJ, Zamorano M, Calero M, Blázquez G (2023) Characterization of the products of the catalytic pyrolysis of discarded COVID-19 masks over sepiolite. Appl Sci 13:3188. https://doi.org/10.3390/appl13053188
32. Serrano-Lotina A, Monte M, Iglesias-Juez A, Pavón-Cadierno AP, Portela R, Ávila P (2019) MnOx-support interactions in catalytic bodies for selective reduction of NO with NH_3. Appl Catal B 256:117821. https://doi.org/10.1016/j.apcatb.2019.117821
33. Zhou F, Yan C, Wang H, Zhou S, Komarneni S (2017) Sepiolite-TiO2 nanocomposites for photocatalysis: synthesis by microwave hydrothermal treatment versus calcination. Appl Clay Sci 146:246–253. https://doi.org/10.1016/j.clay.2017.06.010
34. Degirmenbasi N, Boz N, Kalyon DM (2014) Biofuel production via transesterification using sepiolite-supported alkaline catalysts. Appl Catal B 150:147–156. https://doi.org/10.1016/j.apcatb.2013.12.013
35. Han F, Liu Q, Li D, Ouyang J (2023) An emerging and high-performance sepiolite-supported Ni catalyst for low-temperature CO2 methanation: the critical role of hydroxyl groups. J Environ Chem Eng 11:10331. https://doi.org/10.1016/j.jece.2023.110331
36. Hong YC, Sheng ZM, Hu MH, Dai XY, Chang CK, Chen QZ, Zhang DY (2016) Thin-walled graphitic nanocages with nitrogen-doping as superior performance anodes for lithium-ion batteries. RSC Adv 6:59896–59899. https://doi.org/10.1039/C6RA10803B
37. Balci S (1996) Thermal decomposition of sepiolite and variations in pore structure with and without acid pre-treatment. J Chem Technol Biotechnol 66:72–78
38. González-Pradas E, Socias-Viciana M, Saifi M, Urena-Amate MD, Flores-Cespedes F, Fernández-Pérez M, Villafrenca-Sánchez M (2005) Adsorption of chloridazon from aqueous solution on heat and acid treated sepiolites. Water Res 39:1849–1857
39. Yebra-Rodríguez A, Martín-Ramos JD, Del Rey F, Viseras C, López-Galindo A (2003) Effect of acid treatment on the structure of sepiolite. Clay Miner 38:353–360. https://doi.org/10.1180/0009855033830101
40. Franco F, Pozo M, Cecilia JA, Benítez-Guerrero M, Pozo E, Martín Rubí JA (2014) Microwave assisted acid treatment of

sepiolite: the role of composition and crystallinity. Appl Clay Sci 102:15–27. https://doi.org/10.1016/j.clay.2014.10.013
41. Calero M, Solís RR, Muñoz-Batista MJ, Pérez A, Blázquez G, Martín-Lara MA (2023) Oil and gas production from the pyrolytic transformation of recycled plastic waste: an integral study by polymer families. Chem Eng Sci 271:118569. https://doi.org/10.1016/j.ces.2023.118569
42. Gómez-Avilés A, Belver C, Aranda P, Ruiz-Hitzky E, Clambor MA (2014) Zeolite–Sepiolite nanoheterostructures. J Nanostructure Chem 4:90. https://doi.org/10.1007/s40097-014-0090-5
43. Sun K, Wang C, Zhang G, Niu H, Fu S, Wu Y, Yang J (2020) Adsorption properties of Calcined Modified Sepiolite on SO_4^{2-} and Cl^-. J Wuhan Univ Technol Mater Sci 35:32–41. https://doi.org/10.1007/s11595-020-2223-7
44. Tuler F, Portela R, Ávila P, Bortolozzi JP, Miró E, Milt V (2016) Development of sepiolite/SiC porous catalytic filters for diesel soot abatement. Microporous Mesoporous Mater 230:11–19. https://doi.org/10.1016/j.micromeso.2016.04.026
45. Lin X, Fang J, Chen M, Huang Z, Su C (2016) Co and Fe-catalysts supported on sepiolite: effects of preparation conditions on their catalytic behaviors in high temperature gas flow treatment of dye. Environ Sci Pollut Res 23:15294–15301. https://doi.org/10.1007/s11356-016-6631-3
46. Ardakani MB, Mahabadi HA, Jafari AJ (2019) Catalytic removal of Toluene from Air streams by Cobalt Oxide supported on Sepiolite. J Braz Chem Soc 30:1933–1940. https://doi.org/10.21577/0103-5053.20190106
47. Suárez M, García-Romero E (2012) Variability of the surface properties of sepiolite. Appl Clay Sci 67–68:72–82. https://doi.org/10.1016/j.clay.2012.06.003
48. Yao D, Zhang Y, Williams PT, Yang H, Chen H (2018) Co-production of hydrogen and carbon nanotubes from real-world waste plastics: influence of catalyst composition and operational parameters. Appl Catal B 221:584–597. https://doi.org/10.1016/j.apcatb.2017.09.035
49. Dupin JC, Gonbear D, Vinatierb P, Levasseurb A (2000) Systematic XPS studies of metal oxides, hydroxides and peroxides. Phys Chem Chem Phys 2:1319–1324. https://doi.org/10.1039/a908800h
50. Lv Y, Hao F, Liu P, Xiong S, Luo H (2017) Improved catalytic performance of acid-activated sepiolite supported nickel and potassium bimetallic catalysts for liquid phase hydrogenation of 1,6-hexanedinitrile. J Mol Catal A: Chem 426:15–23. https://doi.org/10.1016/j.molcata.2016.10.029
51. Chen X, Wang S, Qiao G, Wang X, Lu G, Cui H, Wang X (2021) Sepiolite/amorphous nickel hydroxide hierarchical structure for high capacitive supercapacitor. J Alloys Compd 881:160519. https://doi.org/10.1016/j.jallcom.2021.160519
52. Al-Fatesh AS, Al-Garadi NYA, Osman AI, Al-Mubaddel FS, Ibrahim AA, Khan WU, Alanazi YM, Alrashed MM, Alothman OY (2023) From plastic waste pyrolysis to fuel: impact of process parameters and material selection on hydrogen production. Fuel 344:128107. https://doi.org/10.1016/j.fuel.2023.128107
53. Wang J, Zhang J, Zhong H, Wang H, Ma K, Pan L (2020) Effect of support morphology and size of nickel metal ions on hydrogen production from methane steam reforming. Chem Phys Lett 746:137291. https://doi.org/10.1016/j.cplett.2020.137291
54. Zhang Z, Tian Y, Zhang L, Hu S, Xiang J, Wang Y, Xu L, Liu Q, Zhang S, Hu X (2019) Impacts of nickel loading on properties, catalytic behaviors of Ni/γ–Al2O3 catalysts and the reaction intermediates formed in methanation of CO2. Int J Hydrog Energy 44:9291–9306. https://doi.org/10.1016/j.ijhydene.2019.02.129
55. Jiménez-Gómez CP, Cecilia JA, Defilippi C, Maireles-Torres P, Giordano C (2019) Supported nickel nitride catalysts for the gas-phase hydrogenation of furfural. International Symposium on Green Chemistry, 13–17/05/2019, La Rochelle, France. https://riuma.uma.es/xmlui/bitstream/handle/10630/17679/Supported%20nickel%20nitride%20catalysts%20for%20the%20gas_ISGC%20CG.pdf?sequence=3&isAllowed=y
56. Pham CQ, Alsaiari M, Hieu H, Pham PTT, Le Phuong DH, Rajamohan N, Setiabudi HD, Vo DVN, Trinh TH, Pham PTH, Nguyen TM (2024) Efficient methane dry reforming process with Low Nickel Loading for Greenhouse Gas Mitigation. Top Catal 67:748–760. https://doi.org/10.1007/s11244-023-01881-w
57. Carraro PM, Soria FA, Vaschetto EG, Sapag K, Oliva MI, Eimer GA (2019) Effect of nickel loading on hydrogen adsorption capacity of different mesoporous supports. Adsorption 25:1409–1418. https://doi.org/10.1007/s10450-019-00103-8
58. Sharma SS, Batra VS (2019) Production of hydrogen and carbon nanotubes via catalytic thermo-chemical conversion of plastic waste: review. J Chem Technol Biotechnol 95:11–19. https://doi.org/10.1002/jctb.6193
59. Liu X, Zhang Y, Nahil MA, Williams PT, Wu C (2017) Development of Ni- and Fe- based catalysts with different metal particle sizes for the production of carbon nanotubes and hydrogen from thermo-chemical conversion of waste plastics. J Anal Appl Pyrol 125:32–39. https://doi.org/10.1016/j.jaap.2017.05.001
60. Li QL, Shan R, Zhang J, Lei M, Yuan HR, Chen Y (2023) Enhancement of hydrogen and carbon nanotubes production from hierarchical Ni/ZSM-5 catalyzed polyethylene pyrolysis. J Anal Appl Pyrol 169:105829. https://doi.org/10.1016/j.jaap.2022.105829
61. Xu D, Xiong Y, Zhang S, Su Y (2021) The synergistic mechanism between coke depositions and gas for H2 production from co-pyrolysis of biomass and plastic wastes via char supported catalyst. Waste Manag 121:23–32. https://doi.org/10.1016/j.wasman.2020.11.044
62. Alvarez J, Kumagai S, Wu C, Yoshioka T, Bilbao J, Olazar M, Williams PT (2014) Hydrogen production from biomass and plastic mixtures by pyrolysis-gasification. Int J Hydrog Energy 39:10883–10891. https://doi.org/10.1016/j.ijhydene.2014.04.189
63. Wang S, Zhang Y, Shan R, Gu J, Huhe T, Ling X, Yuan H, Chen Y (2022) High-yield H_2 production from polypropylene through pyrolysis-catalytic reforming over activated carbon based nickel catalyst. J Clean Prod 352:131566. https://doi.org/10.1016/j.jclepro.2022.131566
64. Arena U, Mastellone ML, Camino G, Boccaleri E (2006) An innovative process for mass production of multi-wall carbon nanotubes by means of low-cost pyrolysis of polyolefins. Polym Degrad Stab 91:763–768. https://doi.org/10.1016/j.polymdegradstab.2005.05.029
65. Pol VG, Thiyagarajan P (2010) Remediating plastic waste into carbon nanotubes. J Environ Monit 12:455–459. https://doi.org/10.1039/b914648b
66. Kukovitskii EF, Chernozatonskii LA, L'vov SG, Mel'nik NN (1997) Carbon nanotubes of polyethylene. Chem Phys Lett 266:323–328. https://doi.org/10.1016/S0009-2614(97)00020-1
67. Bazargan A, McKay G (2012) A review – synthesis of carbon nanotubes from plastic wastes. Chem Eng J 195–196:377–391. https://doi.org/10.1016/j.cej.2012.03.077
68. Mishra N, Das G, Ansaldo A, Genovese A, Malerba M, Povia M, Ricci D, Fabrizio ED, Zitti ED, Sharon M, Sharon M (2012) Pyrolysis of waste polypropylene for the synthesis of carbon nanotubes. J Anal Appl Pyrol 94:91–98. https://doi.org/10.1016/j.jaap.2011.11.012
69. Wang J, Shen B, Lan M, Kang D, Wu C (2020) Carbon nanotubes (CNTs) production from catalytic pyrolysis of waste plastics: the influence of catalyst and reaction pressure. Catal Today 351:50–57. https://doi.org/10.1016/j.cattod.2019.01.058
70. Modekwe HU, Mamo MA, Moothi K, Daramola MO (2021) Effect of different Catalyst supports on the quality, yield and

morphology of Carbon Nanotubes Produced from Waste Polypropylene Plastics. Catalysts 11:692. https://doi.org/10.3390/catal11060692
71. Nahil MA, Wu C, Williams PT (2015) Influence of metal addition to Ni-based catalysts for the co-production of carbon nanotubes and hydrogen from the thermal processing of waste polypropylene. Fuel Process Technol 130:46–53. https://doi.org/10.1016/j.fuproc.2014.09.022
72. Acomb JC, Wu C, Williams PT (2016) The use of different metal catalysts for the simultaneous production of carbon nanotubes and hydrogen from pyrolysis of plastic feedstocks. Appl Catal B 180:497–510. https://doi.org/10.1016/j.apcatb.2015.06.054
73. Li QL, Shan R, Li WJ, Wang SX, Yuan HR, Chen Y (2024) Co-production of hydrogen and carbon nanotubes via catalytic pyrolysis of polyethylene over Fe/ZSM-5 catalysts: Effect of Fe loading on the catalytic activity. Int J Hydrog Energy 55:1476–1485. https://doi.org/10.1016/j.ijhydene.2023.12.101